https://doi.org/10.5194/egusphere-2025-215
Preprint. Discussion started: 10 February 2025

Isotope discrimination of carbonyl sulfide (^{34}S) and carbon dioxide (^{13}C, ^{18}O) during plant uptake in flow-through chamber experiments

Sophie L. Baartman[1,2], Steven M. Driever[3], Maarten Wassenaar[4], Linda M.J. Kooijmans[2], Nerea Ubierna Lopez[6], Leon Mossink[3], Maria E. Popa[2], Ara Cho[2], Lisa Wingate[6], Thomas Röckmann[1], Steven M.A.C. van Heuven[5], Maarten C. Krol[1,2]

[1]Institute for Marine and Atmospheric Research Utrecht (IMAU), Princetonplein 5, 3584 CC Utrecht, The Netherlands

[2]Meteorology and Air Quality, Wageningen University and Research Centre, Droevendaalsesteeg 4, 6708 PB Wageningen, The Netherlands

[3]Centre for Crop Systems Analysis, Wageningen University and Research Centre, Droevendaalsesteeg 4, 6708 PB Wageningen, The Netherlands

[4]Horticulture and Product Physiology, Wageningen University and Research Centre, Droevendaalsesteeg 4, 6708 PB Wageningen, The Netherlands

[5]Centre for Isotope Research (CIO), Energy and Sustainability Research Institute Groningen, University of Groningen, 9747 AG Groningen, the Netherlands

[6]Institut National de la Recherche Agronomique, Bordeaux Sciences Agro, Unité Mixte de Recherche 1391, Interactions Sol-Plante-Atmosphère, 33140 Villenave d'Ornon, France

Correspondence to: Sophie L. Baartman (sophie.baartman@wur.nl)

Abstract. Carbonyl sulfide (COS) has been proposed as a proxy for gross primary production (GPP), as it is taken up by plants through a comparable pathway as CO_2. COS diffuses into the leaf and undergoes an essentially one-way reaction in the mesophyll cells, catalyzed by the enzyme carbonic anhydrase (CA), and does not exit the leaf again. In order to use COS as a proxy for GPP, however, the mechanisms of COS uptake and its coupling to CO_2 uptake need to be well understood. Characterizing the isotopic discrimination of COS during plant uptake can provide useful information on the COS uptake process and can help to constrain the COS budget.

This study presents joint measurements of isotope discrimination during plant uptake for COS ($CO^{34}S$) and CO_2 ($^{13}CO_2$ and $C^{18}O^{16}O$). A C_3 plant, sunflower (*Helianthus annuus*), and a C_4 plant, papyrus (*Cyperus papyrus*), were enclosed in a flow-through plant chamber and exposed to varying light levels. The incoming and outgoing gas compositions were measured online, and discrete air samples were taken for isotope analysis.

The COS uptake flux was around 75 pmol mol^{-1} for sunflower and between 99 and 110 pmol mol^{-1} for papyrus. The corresponding $^{34}\Delta$ for COS was 3.4 ± 0.8 ‰ for sunflower and 2.6 ± 0.3 ‰ for papyrus. For CO_2, a negative relationship was observed between the uptake flux and the isotopic discriminations $^{13}\Delta$ and $^{18}\Delta$. The CO_2 uptake and Δ values indicate that our sunflower behaved as expected for a C_3 plant, while the papyrus was not displaying typical C_4 behavior, perhaps due to the relative low light conditions during our experiments.

https://doi.org/10.5194/egusphere-2025-215
Preprint. Discussion started: 10 February 2025

1. Introduction

Photosynthetic uptake of CO_2 by the terrestrial biosphere, quantified by the gross primary production (GPP), is the largest sink of atmospheric CO_2, and may be altered as the climate changes. For making accurate future climate projections, it is important to quantify changes in the functioning of the biosphere and its influence on the atmospheric composition. Several techniques can be used to quantify photosynthesis and respiration fluxes at the ecosystem and larger scales, such as Eddy Covariance (EC) (Asaf et al., 2013; Billesbach et al., 2014; Commane et al., 2015; Wehr et al., 2017; Vesala et al., 2022) or variations in the stable isotopic composition of CO_2 (e.g. Farquhar and Lloyd, 1993; Farquhar et al., 1993; Wingate et al., 2007; Gentsch et al., 2014). However, these techniques have limitations, because they either measure net CO_2 fluxes (Wohlfahrt et al., 2012; Kooijmans et al., 2017) or they require additional measurements such as the oxygen isotope composition of water pools (Wingate et al., 2010; Adnew et al., 2020). Because of these limitations, other potential independent proxies for GPP have recently gained attention, especially the trace gas carbonyl sulfide (COS or OCS, COS henceforth) (Whelan et al., 2018; Lai et al., 2024).

COS is the most abundant sulfur-containing atmospheric trace gas, with a tropospheric mole fraction of around 500 ppt that displays a strong seasonal cycle, mostly due to the uptake of COS by terrestrial vegetation during photosynthesis. Figure 1 shows a schematic of the uptake pathways and assimilation locations of COS and CO_2 in the leaf. Similarly to CO_2, COS diffuses across the leaf boundary layer, through the stomata and into the leaf mesophyll cells (Protoschill-Krebs and Kesselmeier, 1992; Protoschill-Krebs et al., 1996). There, COS is hydrolyzed in an essentially one-way reaction, catalyzed by the enzyme carbonic anhydrase (CA), in contrast to the reversible hydration reaction that CO_2 undergoes (Protoschill-Krebs and Kesselmeier, 1992; Protoschill-Krebs et al., 1996). Assuming that there is no COS emission, the COS uptake by plants is proportional to photosynthetic uptake of CO_2, and therefore, GPP can be derived from the leaf-scale relative uptake ratio (*LRU*) of COS and CO_2 uptake fluxes, A^S(pmol m^{-2} s^{-1}) and A^C (µmol m^{-2} s^{-1}), normalized to their atmospheric mole fractions, C_a^S (pmol mol^{-1}) and C_a^C (µmol mol^{-1}) using Eq. (1):

$$LRU = \frac{A^S}{A^C} * \frac{C_a^C}{C_a^S} \tag{1}$$

If we assume negligible daytime leaf respiration, A^C can be replaced by GPP, which can then be estimated using Eq. (2) (re-arrangement of Eq. (1)).

$$GPP = A^S \frac{C_a^C}{C_a^S} * \frac{1}{LRU} \tag{2}$$

While the use of LRU as a link between COS and CO_2 fluxes seems promising, some studies have shown that the LRU is not constant among species and changes with environmental conditions such as photosynthetically active radiation (PAR), temperature and vapor pressure deficit (VPD) (Kooijmans et al., 2019; Maignan et al., 2021; Spielmann et al., 2023; Sun et al., 2024). Thus, a more thorough understanding of the physiological drivers and limitations of COS uptake by plants, and its relationship with CO_2 uptake, is needed.

https://doi.org/10.5194/egusphere-2025-215
Preprint. Discussion started: 10 February 2025

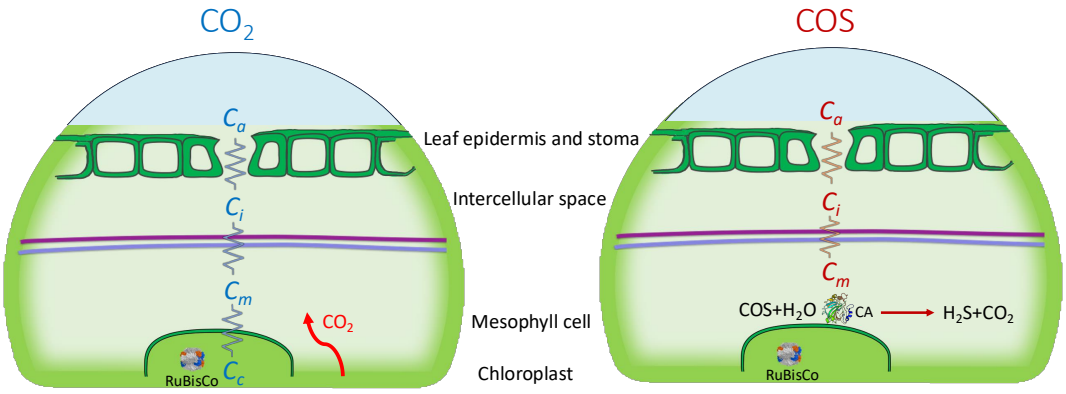

Figure 1. Schematic (simplified) representation of the diffusion pathways of CO_2 (left) and COS (right) into a C_3 leaf, including the mole fractions of both species in the atmosphere (C_a), the intercellular space (C_i), the mesophyll cell (C_m) and, for CO_2, the chloroplast (C_c). The enzymes ribulose-1,5-bifosfaat carboxylase oxygenase (RuBisCo, inside the chloroplast) and carbonic anhydrase (CA, right figure only) catalyze CO_2 and COS fixation.

COS isotope discrimination during plant uptake could provide useful information on the uptake process and its response to environmental factors. The discrimination against $CO^{34}S$ (‰) is defined in Eq. (3), where ^{32}k and ^{34}k are the reaction rate coefficients for uptake of $CO^{32}S$ and $CO^{34}S$, respectively:

$$^{34}\Delta = 1 - \frac{^{34}k}{^{32}k}. \tag{3}$$

Isotope discrimination occurs both during diffusion of COS into the leaf and due to the preferential hydrolysis of lighter isotopologues by CA. Similar to the model developed by Farquhar et al. (1982) for $^{13}CO_2$ discrimination during photosynthesis, the net $CO^{34}S$ discrimination during plant uptake ($^{34}\Delta$) can be expressed as a function of the ratio of COS mole fraction at the site of assimilation (the end-point), in the mesophyll cell (C_m^S) versus the COS mole fraction in ambient air (C_a^S) (Davidson et al., 2022):

$$^{34}\Delta = \bar{a} + (h - \bar{a})\frac{C_m^S}{C_a^S}, \tag{4}$$

where $\bar{a}$ is the fractionation occurring during diffusion of COS into the leaf up to the mesophyll cell, which incorporates leaf boundary layer (BL) diffusion, stomatal diffusion and gas-liquid interface dissolution and diffusion, and h is the S isotope fractionation during fixation by the enzyme carbonic anhydrase (CA).

C_m^S has been suggested to be close to zero in C_3 plants (Stimler et al., 2011; Stimler et al., 2012). When $C_m^S = 0$, Eq. (4) reduces to $^{34}\Delta = \bar{a}$, thus $^{34}\Delta$ is caused solely by diffusion differences between $CO^{32}S$ and $CO^{34}S$ ($\bar{a}$) through the stomata and up to the mesophyll. Binary molecular diffusion of COS in air is theoretically expected to provide a $^{34}\Delta$ value of around 5 ‰, because of the differences in molecular masses between the different COS isotopologues (Angert et al. 2019). However, this may be a too crude simplification of the diffusion processes taking place. When including stomatal diffusion, leaf BL diffusion, and gas–liquid phase diffusion in the mesophyll cell, Davidson et al. (2022) calculated an overall diffusion fractionation value of $\bar{a}$ = 1.6 ± 0.1‰ for ^{34}S.

Still, it is not known whether the COS mole fraction in the mesophyll always reaches values close to zero, especially for C_4 species, in which CA activity is lower (Stimler et al., 2011). In this case, values for the enzymatic

https://doi.org/10.5194/egusphere-2025-215
Preprint. Discussion started: 10 February 2025

fractionation during COS fixation by CA (h) are needed to calculate $^{34}\Delta$. Davidson et al. (2022) determined an enzymatic fractionation for ^{34}S, h, of 15 ± 2 ‰ from experiments in which the plants were exposed to high CO_2 and COS mole fractions.

The observed $^{34}\Delta$ values, measured in C_3 and C_4 species by Davidson et al. (2022), during their series of closed-chamber experiments, were 1.6 ± 0.1 ‰ and 5.4 ± 0.5 ‰, respectively, at ambient COS and CO_2 mole fractions. Here, the higher discrimination value for C_4 species likely reflects the lower CA activity, leading to higher c_m and therefore an influence of b on the observed discrimination.

To date, Davidson et al., (2021) and Davidson et al., (2022) are the only studies that have determined COS isotope discrimination during plant uptake, and they used a closed-chamber approach. As mole fractions of CO_2 and COS change during experiments with closed chambers, there is a potential risk that feedback processes on stomatal conductance and other metabolic processes may contribute to the observed discrimination and hence the results may not reflect typical leaf conditions. With flow-through chambers, conditions can be monitored online and kept stable throughout the entire experiment, also allowing for easier repetition of the experiments.

In this work we used flow-through plant chambers, closely monitored to maintain stable conditions, to perform joint measurements of COS and CO_2 fluxes in C_3 and C_4 species and at a range of PAR. We determined the isotope discrimination of COS uptake against $CO^{34}S$ and CO_2 uptake against $^{13}CO_2$ and $C^{12}O^{18}O$ ($^{34}\Delta$, $^{13}\Delta$, and $^{18}\Delta$). The joint COS and CO_2 measurements allowed investigating the relationship between COS and CO_2 isotope effects, where the CO_2 data provide additional information for validating the experimental setup and the plant behavior.

2. Methods

2.1. Plant materials and growing conditions

Experiments were conducted with the C_3 plant sunflower (*Helianthus Annuus* "Sunsation") and the C_4 plant papyrus (*Cyperus papyrus*). Sunflower plants in the flowering stage were obtained at a local garden center. In the case of papyrus, three large stems with leaves were carefully cut using a sharp razor, from a larger shrub growing in the tropical greenhouse at Wageningen University and Research (WUR). These leaves were transported with their cut stem in water to the lab and kept in water throughout the chamber measurements. The sunflower plant and papyrus cuttings were kept under a lamp with a solar-like spectrum (*ca*. 400 µmol m^{-2} s^{-1} PAR, LED growth light SMD2835, Ortho, China) before experiments started and watered sufficiently before and during the measurements. Leaf surface area of sunflower and papyrus were measured after the experiments using a LI-3100 (Li-Cor, Lincoln, NE, USA). This instrument was calibrated using a metal disk with a surface area of exactly 50.00 cm^2.

2.2. Whole plant gas exchange system

Gas exchange experiments were conducted at Wageningen University and Research (WUR) using a custom-built whole plant chamber that was developed for estimating net photosynthetic CO_2 assimilation and transpiration (Lazzarin et al., 2024). The main component is a flow-through plant chamber, which can be fed with different gas mixtures. Two analyzers were used to measure in- and outgoing mole fractions and we used an add-on module for discrete air samples (Fig 2.).

https://doi.org/10.5194/egusphere-2025-215
Preprint. Discussion started: 10 February 2025

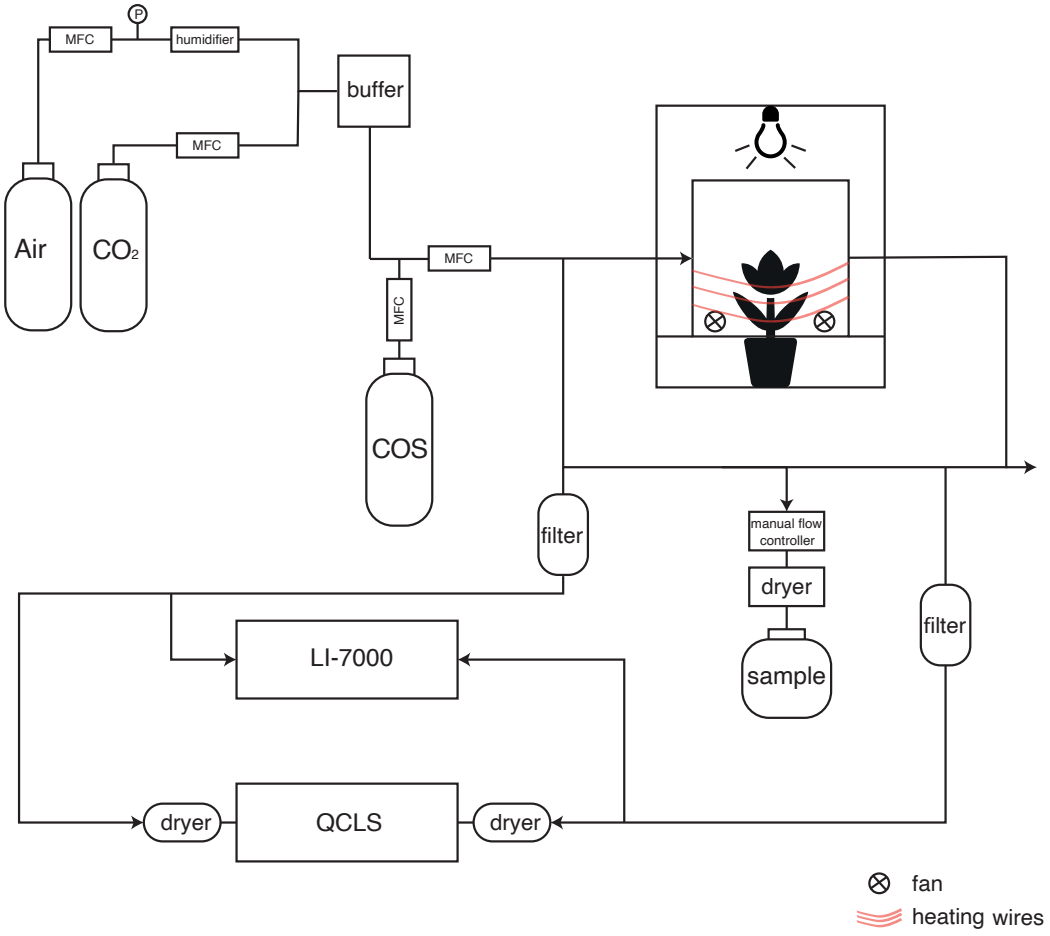

Figure 2. Schematic overview of the setup to determine CO_2 and COS photosynthetic isotope discrimination by coupling a custom-built plant chamber to a LI-7000, a QCLS and a system to fill up gas canisters for posterior isotope analysis with IRMS. MFC: mass flow controller; QCLS: Quantum Cascade Laser Spectrometer. CO_2 and COS were mixed into humidified synthetic air and introduced into the plant chamber. The in- and outflowing airstreams of the chamber (air_{in} and air_{out}) were measured by both the LI-7000 and QCLS instruments. Air was dried using $Mg(ClO_4)_2$ before the QCLS and when taking a sample for isotope analysis.

The plant chamber was made of clear plexiglass lined with a FEP foil (Holscot Europe, Breda NL) to prevent water from sticking to the chamber walls. The chamber had a diameter of 29 cm, and the height was either 18 or 27 cm, depending on the plant size. To ensure proper air mixing and leaf boundary layer reduction, three SanAce40W ventilators (type 9WL0424P3J001, Sanyo120 Denki, Philippines) were placed in a circular pattern at the bottom of the chamber. Fan speed was controlled with a SanAce PWM controller. The entire chamber was placed inside a 63x63 cm^2 enclosure with white reflective walls that ensured uniform horizontal light distribution. Air temperature inside the plant chamber was measured with a LM35 temperature sensor (Texas Instruments). Temperature of the plant chamber was controlled using heating cables positioned around the outside of the plant chamber (in combination with a PID controller) and two 12V computer fans were used to provide airflow and cooling around the plant chamber. Light was

https://doi.org/10.5194/egusphere-2025-215
Preprint. Discussion started: 10 February 2025

provided by LED lighting mounted above the chamber with a spectrum resembling sunlight (artificial sunlight research modules generation 2, Specialty Lighting Holland B. V., Breda, the Netherlands). PAR was quantified during the experiments just above the chamber using a handheld PAR sensor (LI-190, Li-Cor, Lincoln, NE, USA). Plants were placed in the chamber, and the bottom two plexiglass panels were closed around the stem of the plant and sealed it with Terostat RB VII, ensuring that the plant was isolated from the soil or water (in the case of the papyrus), and making sure the chamber was leak-free. Two pictures of the plant chamber are shown in Appendix A, Fig. A2.

Synthetic air humidified with a temperature-controlled water bubbler (dew point temperature 17 °C) was mixed with pure CO_2 using mass flow controllers (MFC), to reach the desired CO_2 and H_2O mole fractions. Subsequently, COS from a cylinder with 700 ppb COS in synthetic "zero" air was supplied to the mix using a MFC to establish the target COS mole fractions of approximately 2 ppb. The flow rate of the total (combined) air mixture into the chamber was controlled by a MFC to around 8 L min^{-1}, depending on the experiment conducted. The COS and CO_2 isotopic composition of the ingoing air was determined using the methods described in 2.5 and the values are provided in Table 1.

Table 1. Isotope composition of the inlet gas (air_{in}) supplying the plant chamber determined from samples collected in canisters and analyzed with IRMS.

Plant	**δ^{34}S COS (‰)**	**δ^{13}C CO_2 (‰)**	**δ^{18}O CO_2 (‰)**
Sunflower	11.9 ± 1.2	–23.1 ± 0.1	15.5 ± 0.1
Papyrus	12.1 ± 0.5	–23.0 ± 0.1	15.9 ± 0.1

The CO_2 and H_2O mole fractions of both the in-going air (air_{in}, reference line) and the outgoing air (air_{out}, sample line) of the chamber were analyzed with a LI-7000 infrared gas analyzer (LI-COR Biosciences, Lincoln, Nebraska, USA). CO_2 and COS mole fractions of the air_{in} (reference) and air_{out} (sample) lines were also measured with a QCLS from the Center for Isotope Research, Rijksuniversiteit Groningen (CIO-RUG). The QCLS used a 50 mL min^{-1} flow and was manually switched between air_{in}, air_{out} and calibration cylinders. The air entering the QCLS was dried with magnesium perchlorate ($Mg(ClO_4)_2$) dryers. Calibration of the QCLS was performed at least twice a day using the working standards from the CIO-RUG, which are calibrated against NOAA-certified cylinders. Possible instrumental baseline drift during the experiments was corrected by measuring pure nitrogen (N_2) multiple times during the experiment. For a detailed description of the QCLS instrument and calibration procedures, see Kooijmans et al. (2017).

Samples for isotope analysis were taken in 6 L evacuated Silonite canisters (ENTECH, type: PN: 29- 10622) that were filled to ambient pressure. Sampling was done through a $Mg(ClO_4)_2$ dryer and a filter, and the flow into the canisters was regulated using a manual flow controller. The dryer was changed after every two samples. Sampling for COS and CO_2 isotope composition started after ingoing and outgoing concentrations had stabilized, to ensure stable rates of photosynthesis, respiration, and COS assimilation. The stability of these fluxes, prior to sampling, was assured by checking the online data of the QCLS and LI-7000.

2.3. Experimental conditions

For all experiments the chamber was supplied with air mixtures with [COS] = 2300–2400 ppt, and [CO_2] = 430–440 ppm at a flow rate of 8.1 L min^{-1}, giving an air residence time of around 1.5–2 min. Temperature in the chamber was

https://doi.org/10.5194/egusphere-2025-215
Preprint. Discussion started: 10 February 2025

24.6–25.0 °C in sunflower experiments and 25.7–25.9 °C in papyrus experiments. Light intensity was sequentially set to PAR = 400, 600, 200, and 0 µmol m^{-2} s^{-1}, allowing time after each light setting for plant adjustment, uptake flux stabilization and subsequent isotope sampling. Measurements at PAR 600 µmol m^{-2} s^{-1} were not performed with the papyrus due to time constrains. At the start of each experiment with a new plant, two samples were taken of the in-going air (air$_{in}$). Samples were collected in 6 L canisters from air$_{in}$ (at the start of each experiment with a new plant) and air$_{out}$ (at each light setting). For the dark measurements chamber light was switched off and the chamber was covered with a blanket.

2.4. Uptake flux calculations

Both CO_2 and COS net uptake fluxes (A^s in pmol m^{-2}s^{-1} and A^C in µmol m^{-2}s^{-1}) were calculated using Eq. (5) (which shows the calculation for COS):

$$A^s = \frac{u_e}{S}\left(c_e^s - c_a^s \frac{1-w_a}{1-w_o}\right), \tag{5}$$

where u_e is the molar flow of air entering the chamber (mol air s^{-1}), S is the leaf area (m^2), and w_e and w_a (mol of H_2O mol air^{-1}) are the mole fractions of water vapor in air$_{in}$ and air$_{out}$, c_e^s and c_o^s (pmol COS mol air^{-1}) are the [COS] in air$_{in}$ and air$_{out}$, respectively.

The uncertainties of the uptake fluxes were calculated by propagating the uncertainties of the in- and out-going air mole fraction measurements. In the case of the mole fraction measurements by the QCLS, the 1σ uncertainties were obtained from measurements during which either air$_{in}$ or air$_{out}$ was being measured, which was usually around 15 minutes.

As a consistency check, we also calculated the uptake fluxes using the CO_2 and COS mole fractions determined with the mass spectrometer in the canister samples. Comparison of fluxes determined by both methods lead to the exclusion of two samples because of suspected contamination (see Fig. A1 in Appendix A). QCLS COS and CO_2 fluxes, excluding these two samples, were used in subsequent analyses.

From the CO_2 fluxes, the water vapor fluxes obtained from the LI-7000 analyzer and the leaf temperature, we calculated C_i^C/C_a^C using the gas exchange calculations by Farquhar et al. (1980) (details in Appendix B). The leaf internal COS mole fraction, C_i^S, was calculated using Eqs. (6) and (7), including a ternary correction:

$$C_i^S = \frac{\left(g_t^s - \frac{E}{2}\right)c_a^s - A^s}{g_t^s + \frac{E}{2}}, \tag{6}$$

where g_t^s is the total leaf conductance to COS from ambient air to the internal leaf space (C_i) (Eq. (7)).

$$g_t^s = \frac{1}{\frac{1.94}{g_s^w} + \frac{1.56}{g_b^w}} \tag{7}$$

Here, g_b^w is the boundary layer conductance to water, which was assumed infinite, as the ventilators created a well-mixed chamber. The coefficients 1.94 and 1.56 (mol H_2O mol COS^{-1}) are the ratios of diffusivities of COS to water vapor in air and the boundary layer, respectively (Fuller et al., 1966; Farquhar & Lloyd, 1993).

From the $CO^{34}S$ isotope discrimination values ($^{34}\Delta$, Eq. (4)), we estimated the COS mole fraction in the mesophyll cell (C_m^S), using Eq. (8).

https://doi.org/10.5194/egusphere-2025-215
Preprint. Discussion started: 10 February 2025

$$c_m^s \cong \frac{c_a^s(\Delta^{34}S - a_b) + c_s^s(a_b - a_s) + c_i^s(a_s - a_m)}{h - a_m}, \quad (8)$$

where the diffusion fractionation components of $\bar{a}$ were split into fractionation occurring during boundary layer diffusion ($a_b = 3.5$ ‰), stomatal diffusion ($a_s = 5.2$ ‰) and mesophyll diffusion ($a_m = 0.5$ ‰). h (=15 ‰) is again the fractionation occurring during COS hydrolysis by CA (Eq. (4)). The estimated values for these fractionations are from Davidson et al., (2022). Further details and the derivations of these calculations can be found supplementary material S3.

2.5. Isotope ratio measurements

COS and CO_2 isotope ratios in the canister samples were determined using isotope ratio mass spectrometry (IRMS) at Utrecht University. Before measurement, the sample canisters' pressure was increased by adding COS-free zero air, as the extraction system needs overpressure. The $\delta^{34}S$ in COS was determined according to the methods described in Baartman et al. (2021) but using a new Delta V Plus mass spectrometer, which was specifically customized to measure COS isotope ratios and therefore had improved performance (Thermo Fisher Scientific, USA). The continuous-flow GC-IRMS system measures the S^+ fragment ions generated in the IRMS ion source by the electron-impact fragmentation of COS. The isotope ratios were calculated relative to our laboratory standard, which is a 50 L cylinder, filled with outside air and spiked with COS to approximately 800 ppt COS. This lab standard was calibrated against the Vienna Canyon Diablo Triollite (VCDT) international sulfur isotope standard (see Baartman et al., 2021 for a detailed description of the COS isotope measurement system). The typical reproducibility error for $\delta^{34}S$ in COS was 0.4 ‰ and the typical uncertainty for a single sample measurement with ambient COS mole fraction was 0.9 ‰ (Baartman et al., 2021).

The $\delta^{13}C$ and $\delta^{18}O$ in CO_2 were measured using a separate continuous flow IRMS system, initially developed for measuring CO isotopologues (Pathirana et al. 2015), and later modified to measure CO_2 isotopologues. A laboratory reference air cylinder with known isotopic composition was used for calibration (Brenninkmeijer, 1993). Typical precision was better than 0.2 ‰ for both $\delta^{13}C$ and $\delta^{18}O$. Values are reported on the Vienna Pee Dee Belemnite (VPDB) ($\delta^{13}C$) and Vienna Standard Mean Ocean Water (VSMOW) ($\delta^{18}O$) scales. The COS and CO_2 isotopic compositions of the gas entering the chamber are given in Table 1.

2.6. Isotope discrimination calculations

Observed isotope discrimination (‰) was calculated using Eqs. (9) and (10) (Evans et al. 1986):

$$\Delta = \frac{\xi(\delta_{out} - \delta_{in})}{1000 + \delta_{out} - \xi(\delta_{out} - \delta_{in})}, \quad (9)$$

where δ_{in} and δ_{out} are the isotope compositions of the gas entering and leaving the chamber, respectively, for the gas of interest ($\delta^{13}C$, $\delta^{18}O$ in CO_2, or $\delta^{34}S$ in COS). ξ is calculated as:

$$\xi = \frac{c_{in}}{c_{in} - c_{out}}, \quad (10)$$

where c_{in} and c_{out} are the mole fractions of the gas of interest (in our case CO_2 or COS), entering and leaving the chamber, respectively. At the start of each experiment, two canister samples were collected from the chamber inlet and their average was used to characterize air_{in} (c_{in} and δ_{in}, Table 1), which was assumed constant over the experiment as it was supplied from a cylinder.

https://doi.org/10.5194/egusphere-2025-215
Preprint. Discussion started: 10 February 2025

The errors on the measured mole fractions and isotope ratios were propagated to the isotope discrimination values (Δ); details are provided in the supplementary material.

Table 2. Isotope composition of the inlet gas (air_{in}) supplying the plant chamber determined from samples collected in canisters and analyzed with IRMS.

Plant	$\delta^{34}S$ COS (‰)	$\delta^{13}C$ CO_2 (‰)	$\delta^{18}O$ CO_2 (‰)
Sunflower	11.9 ± 1.2	–23.1 ± 0.1	15.5 ± 0.1
Papyrus	12.1 ± 0.5	–23.0 ± 0.1	15.9 ± 0.1

3. Results and Discussion

3.1. COS and CO_2 uptake fluxes

In experiments with both plant species there was a net uptake of COS under all light conditions, including dark (Fig. 3b). Mean COS uptake fluxes in the light were 74.2 ± 1.5 pmol m^{-2} s^{-1} and 109.2 ± 5.5 pmol m^{-2} s^{-1} for sunflower and papyrus, respectively, and uptake fluxes did not vary strongly for different light conditions. Note that samples in the dark were taken sequentially, when plant conditions were still adjusting. Therefore, these samples were not treated as duplicates. As hydrolysis of COS, catalyzed by CA, is a light-independent reaction, COS assimilation can continue as long as the stomata are open (Protoschill-Krebs et al., 1996). Previously reported COS uptake fluxes at canopy- or ecosystem scale usually range between 30 and 60 pmol m^{-2} s^{-1} (Cho et al., 2023; Kooijmans et al., 2017; Commane et al., 2015; Billesbach et al., 2014), with some higher reported uptake fluxes around 80 to 100 pmol m^{-2} s^{-1} (Asaf et al., 2013; Spielmann et al., 2023). Thus, our measured COS uptake fluxes are at the high end of the spectrum, which may be due to the high ambient COS mole fraction inside the chamber.

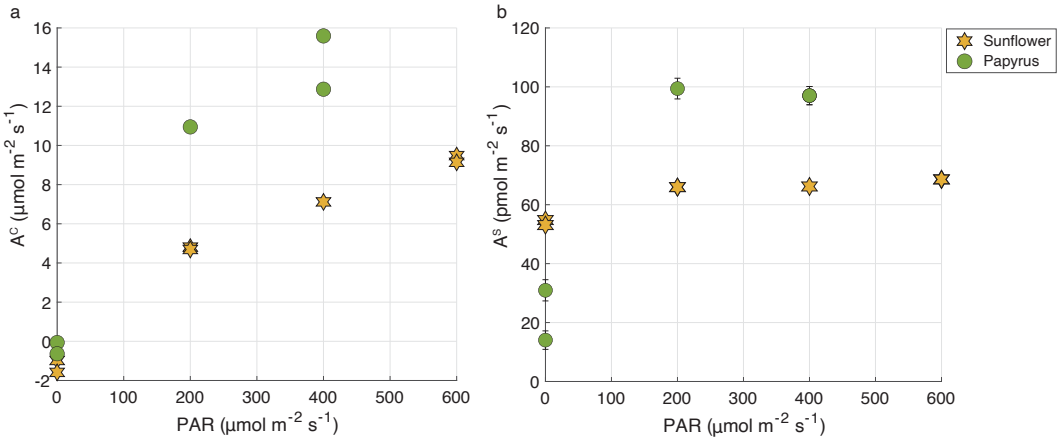

Figure 3. A^C (CO_2 uptake flux, panel a, in µmol m^{-2} s^{-1}) and A^S (COS uptake flux, panel b, in pmol m^{-2} s^{-1}) versus (PAR, µmol m^{-2} s^{-1}) for sunflower (orange stars) and papyrus (green circles). Flux values for PAR > 0 are means ± 1 standard error (SE) (n = 2), where 1 SE was obtained using error propagation (see supplementary materials), flux values for PAR = 0 reflect individual measurements. Errors are only displayed when larger than the symbols.

For CO_2, both sunflower and papyrus performed CO_2 respiration in the dark and photosynthesis in the light, at a net rate that increased with PAR (Fig. 3a). Mean CO_2 uptake fluxes in light conditions were 6.7 ± 1.7 µmol m^{-2}

https://doi.org/10.5194/egusphere-2025-215
Preprint. Discussion started: 10 February 2025

s^{-1} for sunflower and 11.7 ± 2.2 µmol m^{-2} s^{-1} for papyrus (Fig. 3a). These photosynthesis rates match that of sunflowers of Tezera et al. (2008) under their low-light condition experiments (in the least drought-exposed conditions).

At all light intensities (PAR>0), CO_2 uptake rates were larger in papyrus than in sunflower, matching expectations for C_4 vs. C_3 photosynthesis (Farquhar & Lloyd, 1993). The photosynthesis rates for papyrus are comparable with previous measurements, conducted under low-light conditions. Our measurements can be classified as relatively low-light, because although the PAR measured at the top of the chamber reached 400 µmol m^{-2} s^{-1} at the highest setting for the C_4 experiments, the PAR that was received by the plant leaves was likely lower, especially considering that some leaves were (partially) shaded or received diffused light, reflected off the outer enclosure walls. Ubierna et al., (2013) also found CO_2 assimilation rates of around 10 µmol m^{-2} s^{-1} for PAR levels of 500 µmol m^{-2} s^{-1} in three C_4 species, *Zea mays*, *Miscanthus* x *giganteus* and *Flaveria bidentis*, under varying light conditions between 0 and 2000 µmol m^{-2} s^{-1}. Their results are similar to our measured CO_2 uptake fluxes of between 9.4 µmol m^{-2} s^{-1} (200 PAR) and 14.0 µmol m^{-2} s^{-1} (400 PAR).

At PAR = 600 µmol m^{-2} s^{-1}, LRU (Eq. (1)) was 2.3 for sunflower and at PAR = 400 µmol m^{-2} s^{-1}, LRU values were 3.0 and 1.6 for sunflower and papyrus, respectively (see Table 2.). As PAR decreased to 200 µmol m^{-2} s^{-1}, LRU increased to 5.2 for sunflower and 3.0 for papyrus. The increase in LRU at low light was due to a decrease in CO_2 uptake fluxes while the COS uptake remained roughly constant. In the dark, LRU values were negative, up to –16.0 for sunflower, as COS uptake by the plant continued while CO_2 was being respired. Our LRU values are higher than those found by Stimler et al. (2011) and higher than the usually reported median LRU value of 1.7 (Whelan et al., 2018), which may be due to our relatively low-light experiments. Yet, previously reported LRU values vary between 0.7 and 6.2, and Stimler et al. (2011) also reported a higher LRU for C_4 compared to C_3. Our slightly high LRU values could also be due to the higher than ambient COS mole fractions (of around 2ppb) that the plants were exposed to during our experiments. Davidson et al. (2022) reported LRU values or 0.7 and 1.7 for C_3 and C_4, respectively for experiment with ambient COS mole fractions, and LRU values of 2.4 and 1.0 for C_3 and C_4 for plants exposed to 2900 ppm CO_2 and 3.4 ppb COS. Thus, exposure to higher COS mole fractions could influence LRU, however, more research is needed to quantify this effect. Furthermore, recent research has shown that LRU can differ across species and vary with environmental conditions, especially light availability and VPD (Kooijmans et al., 2019; Spielmann et al., 2023). The exact mechanism for this varying LRU is still not completely understood (Whelan et al., 2018; Wohlfahrt et al., 2023).

Figure 4 shows the CO_2 uptake flux (µmol m^{-2} s^{-1}) versus C_i^C/C_a^C ratio, which increases with decreasing CO_2 uptake flux for both species. The species differences in CO_2 uptake flux are consistent with the results presented by Stimler et al. (2011). Our measured C_i^C/C_a^C for sunflower compares well with previous values for sunflower of 0.8 found by Tezara et al. (2008). The c_i/c_a for papyrus is generally high for a C_4 species, for which values usually range around 0.4, but could again be explained by the low-light conditions, as previously observed by Ubierna et al., (2013). The higher than usual C_i^C/C_a^C could also be explained by the fact that we measured entire plants, of which some leaves were partly shaded.

https://doi.org/10.5194/egusphere-2025-215
Preprint. Discussion started: 10 February 2025

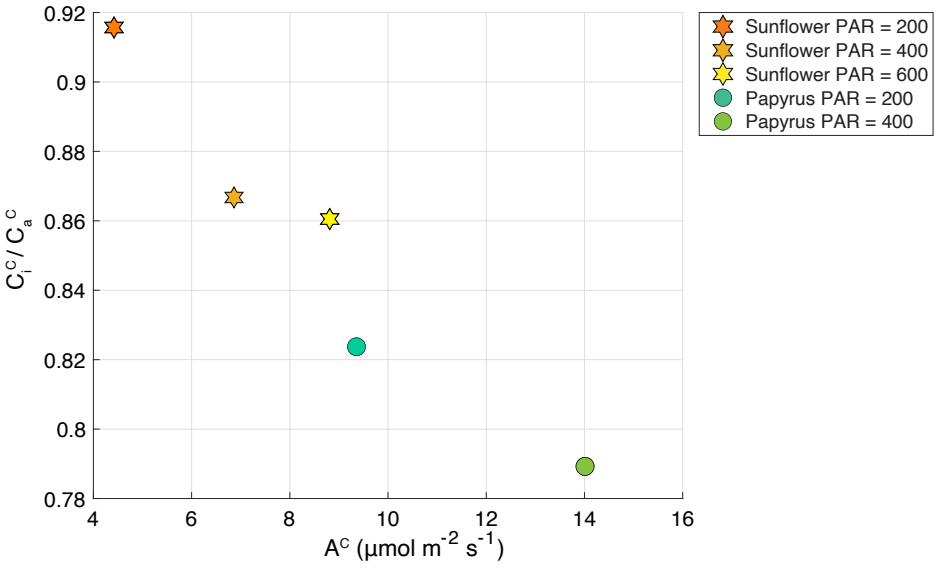

Figure 4. C_i^C/C_a^C plotted against A^C (CO_2 uptake flux in µmol m^{-2} s^{-1}), for sunflower (stars) and papyrus (circles). Colors indicate PAR levels (µmol m^{-2} s^{-1})

3.2 CO^{34}S discrimination

Table 2 shows the isotopic discrimination for COS ($^{34}\Delta$) and CO_2 ($^{13}\Delta$, $^{18}\Delta$), and accompanying data for the different light treatments. In contrast to the CO_2 isotope discrimination (Sect. 3.3), $^{34}\Delta$ did not show a trend with COS uptake flux and PAR (Fig. 5), C_i^S/C_a^S (Fig. 6) or species. The average $^{34}\Delta$ values in light conditions (PAR>0) were 3.4 ± 0.8 ‰ for sunflower and 2.6 ± 0.3 ‰ for papyrus (see Table 2). For sunflower in dark conditions, we found a $^{34}\Delta$ of 4.7 ‰ for the first sample and 1.3 ‰ for the second sample, giving an average $^{34}\Delta$ of 3.0 ± 2.3 ‰ . The COS uptake flux for papyrus in dark conditions decreased drastically to the point that $^{34}\Delta$ could no longer be estimated with confidence.

Table 3. Photosynthetic discrimination (mean ± 1σ, n=2), COS and CO_2 uptake fluxes (A^S and A^C), LRU, C_i^S/C_a^S and C_m^S/C_a^S for sunflower and papyrus, for each PAR level. The uncertainties were calculated as the standard deviation of the mean and the student's t-distribution, with 60% confidence interval and 1 (=n–1) degree of freedom. Values without stated uncertainty are single sample measurements (in the case of isotope discrimination values) or have an uncertainty smaller than 0.01(in the case of A^s, C_i^S/C_a^S and C_m^S/C_a^S). A^S at PAR = 0 for papyrus was too small for calculating $^{34}\Delta$.

Plant	PAR (µmol m^{-2} s^{-1})	$^{34}\Delta$ (‰)	$^{13}\Delta$ (‰)	$^{18}\Delta$ (‰)	A^S (µmol m^{-2} s^{-1})	A^C (pmol m^{-2} s^{-1})	LRU	C_i^S/C_a^S	C_m^S/C_a^S
Sunflower	200	3.6 ± 1.2	32.4 ± 1.1	148.7 ± 0.7	72.1	4.42	5.2	0.50	0.11
Sunflower	400	3.7	24.9	83.6	72.3	6.86	3.1	0.52	0.07
Sunflower	600	2.8 ± 0.6	23.6 ± 1.2	63.8 ± 0.9	74.9	8.81	2.3	0.62	0.04

https://doi.org/10.5194/egusphere-2025-215
Preprint. Discussion started: 10 February 2025

[a]Sunflower	0	3.0 ± 2.3	-	-	59.0 ± 1.31	-	-	0.45	-
Papyrus	200	2.5	21.8	79.4	108.6	9.36	3.0	0.39	0.05
Papyrus	400	2.6 ± 0.4	18.9 ± 3.4	49.4 ± 0.4	105.9	14.01	1.7	0.58	0.03
Papyrus	0	-	-	-	24.6 ± 13.1	-	-	0.72 ± 0.16	

[a]There was no uptake of CO_2 at PAR = 0

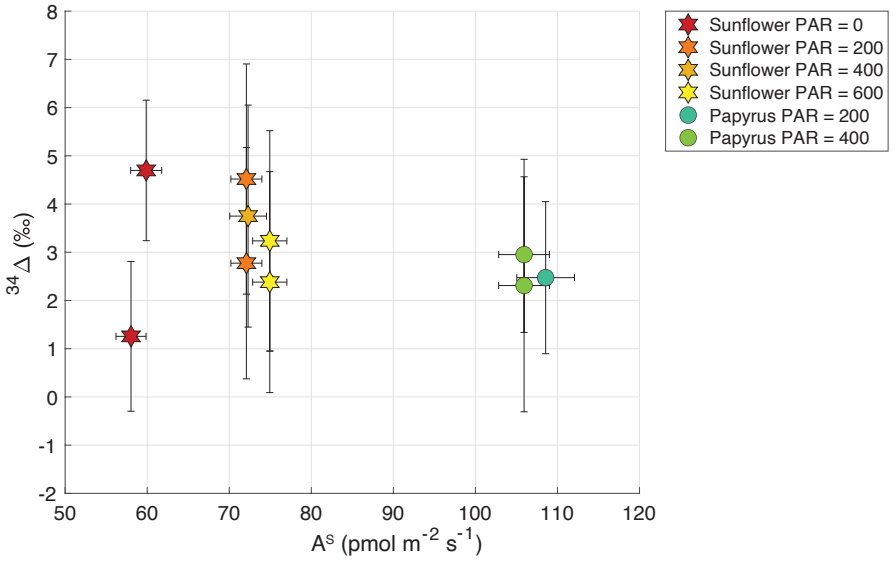

Figure 5. Plant COS isotope discrimination ($^{34}\Delta$) plotted against A^S (COS uptake flux in pmol m^{-2} s^{-1}) for sunflower (stars) and papyrus (circles). Colors indicate PAR levels (µmol m^{-2} s^{-1}).

https://doi.org/10.5194/egusphere-2025-215
Preprint. Discussion started: 10 February 2025

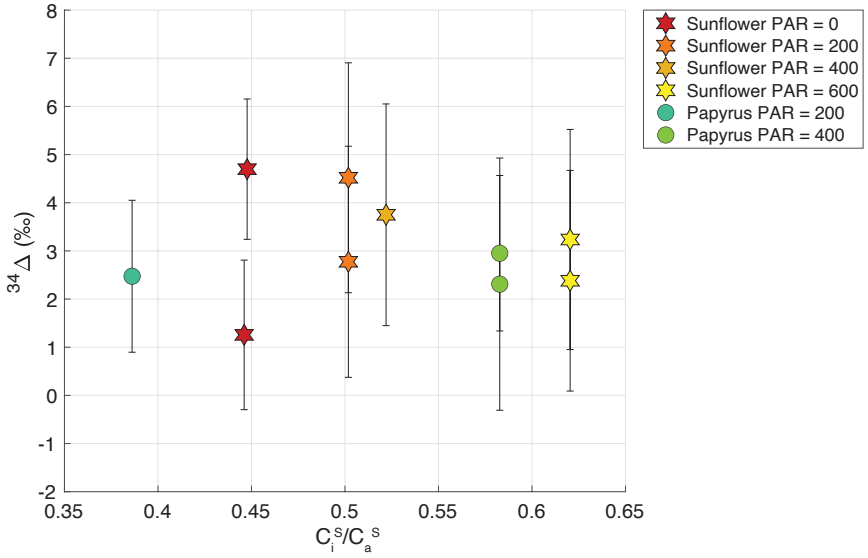

Figure 6. Plant COS isotope discrimination ($^{34}\Delta$) against the ratio of internal versus C_i^S/C_a^S, for sunflower (stars) and papyrus (circles). Colors indicate PAR levels (µmol m^{-2} s^{-1}).

To further investigate this lack of variability in $^{34}\Delta$, we examine the variability in C_i^S/C_a^S and C_m^S/C_a^S as a function of PAR (Table 2). We observed a slight increase of C_i^S/C_a^S with PAR, indicating that the stomata were perhaps not at their maximum opening at PAR≤400, which was also suggested by the CO_2 assimilation and isotope discrimination results (Figs. 4 and 7). However, C_m^S/C_a^S was rather stable at low values around 0.1– 0.23 over the various PAR levels and did not differ substantially between sunflower and papyrus. This lack in variability in C_m^S/C_a^S could explain the absence in variability in $^{34}\Delta$ across the different light settings and between the two measured species, as previous studies (Stimler et al., 2011; Davidson et al., 2021; Davidson et al., 2022) attribute the differences in isotope discrimination between C_3 and C_4 species to differences in C_m^S/C_a^S.

Angert et al. (2019) estimated a value for $^{34}\Delta$ during COS plant uptake of around 5 ‰ (based on binary diffusion theory), and experiments presented by Davidson et al. (2021) and Davidson et al. (2022) yielded $^{34}\Delta$ values of 1.6 ± 0.1 ‰ for C_3 and 5.4 ± 0.5 ‰ for C_4 species. These are the only studies on COS isotope discrimination during plant uptake that have been conducted to date. Our results differ from these measurements, and we did not find statistically different $^{34}\Delta$ values between our C_3 and C_4 species. The $^{34}\Delta$ of 2.8 to 3.7 ‰ that we measured for sunflower is in between the $^{34}\Delta$ for C_3 found by Davidson et al. (2021; 2022) and the theoretical estimate of Angert et al. (2019). However, all $^{34}\Delta$ estimations are roughly in the same range, which is reassuring given that different measurement techniques were used (flow-through chamber compared to closed-chamber).

The benefit of using a flow-through system is that stable environmental conditions inside the chamber can be maintained during the experiment. In contrast, in a closed chamber, CO_2 and COS mole fractions will decrease due to plant uptake, which can be problematic when the experiment runs over long periods of time. Furthermore,

https://doi.org/10.5194/egusphere-2025-215
Preprint. Discussion started: 10 February 2025

transpiration by the plant will increase the water vapor mole fraction in the chamber, which might affect stomatal opening and therefore also the isotope fractionation.

3.3 CO_2 isotope discrimination

3.3.1 $^{13}CO_2$ discrimination

In both sunflower and papyrus, $^{13}\Delta$ increased as the CO_2 uptake flux decreased, with decreasing PAR (Fig. 7). Average $^{13}\Delta$ in sunflower was between 23.6 and 32.4 ‰ (Table 2), which is within the range of values expected for C_3 photosynthesis (Farquhar et al. 1982, Kohn 2010, Cernusak et al. 2013, Wingate et al., 2007). However, in papyrus, $^{13}\Delta$ was between 18.9 and 21.8 ‰; much larger than the expected 3–6 ‰ for C_4 species operating at optimal conditions (Farquhar et al 1983; Cerling et al. 1997; Kubásek et al., 2013; Ellsworth and Cousins, 2016; Eggels et al., 2021). As previously explained, our measurements were performed at low light intensities (PAR≤400 µmol m^{-2} s^{-1}), which resulted in moderately low photosynthetic rates (9.3–14.0 µmol m^{-2} s^{-1}). In C_4 species, $^{13}\Delta$ has been shown to increase at low light to values as large as 8–17‰, when PAR = 50–125 µmol $m^{-2}s^{-1}$ (Ubierna et al. 2013, Pengelly et al. 2010, Kromdijk et al. 2010) and photosynthetic rates were small (<5 µmol $m^{-2}s^{-1}$). Our $^{13}\Delta$ values for papyrus are still larger than these previous reports at low irradiance, suggesting that processes other than photosynthesis might have affected the measurements. Upward transport of water dissolved CO_2 in the transpiration stream has been shown in tree stems (Aubrey and Teskey, 2009; Bloemen et al. 2013) and in papyrus culms (Li and Jones, 1995). We measured detached papyrus leaves submerged in water. This setting could have facilitated the transport of water dissolved CO_2 into the leaf chamber, particularly because papyrus leaves have numerous vascular bundles surrounded by large air cavities (Plowman, 1906). Water dissolved CO_2 would presumably have near-ambient air $\delta^{13}C$ values – enriched compared to tank CO_2 supplied to the chamber air –, and therefore if released in the plant chamber would artefactually increase $^{13}\Delta$.

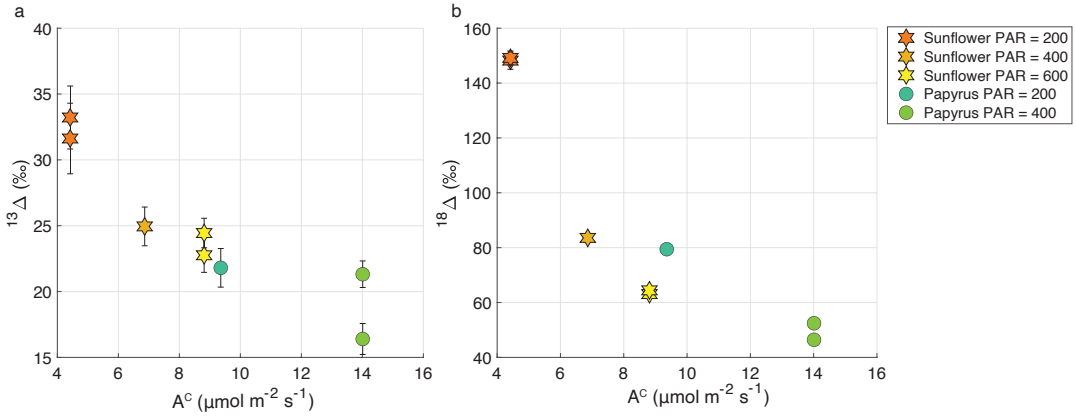

Figure 7. Variation of photosynthetic discrimination against $^{13}CO_2$ ($^{13}\Delta$, panel a) and $CO^{18}O$ ($^{18}\Delta$, panel b) as a function of A^C (CO_2 uptake flux in µmol m^{-2} s^{-1}) for sunflower (stars) and papyrus (circles). Colors indicate PAR levels (µmol m^{-2} s^{-1}).

3.3.2 $C^{16}O^{18}O$ discrimination

https://doi.org/10.5194/egusphere-2025-215
Preprint. Discussion started: 10 February 2025

From Fig. 7, we observe a negative relationship between $^{18}\Delta$ and CO_2 uptake flux, similar to $^{13}\Delta$. The average $^{18}\Delta$ values of sunflower range between 63.8 and 148.7 ‰ and the average $^{18}\Delta$ values of papyrus are between 49.4 and 79.4 ‰ (Table 2). Thus, the $^{18}\Delta$ of papyrus is clearly lower than that of sunflower. $^{18}\Delta$ mostly reflects the exchange of ^{18}O between CO_2 and leaf water (Francey and Tans; Yakir, 1998; Adnew et al., 2020). The lower $^{18}\Delta$ in C_4 species likely indicates the incomplete equilibrium between CO_2 and leaf water, because of the reduced CA activity in C_4 species compared to most C_3 species (Gillon and Yakir, 2000).

A negative correlation of $^{18}\Delta$ with CO_2 assimilation and light intensity, as well as lower $^{18}\Delta$ in C_4 species was also found by Stimler et al. (2011). For their C_3 plants, they found an $^{18}\Delta$ which ranged between around 40 and 240 ‰, where the highest values were found at the lowest CO_2 uptake fluxes. For C_4 species, Stimler et al. (2011) found an $^{18}\Delta$ between 10 and 50 ‰. Seibt et al. (2006) also found large variations in $^{18}\Delta$ during CO_2 uptake by *Picea sitchensis*, and a correlation with PAR. They too measured the largest $^{18}\Delta$ discrimination at dusk and dawn, when light intensity was lowest.

The relation between the COS uptake flux and $^{18}\Delta$ can also be analyzed, since both depend on the same diffusion pathway and CA activity (Stimler et al., 2011). Stimler et al. (2011) observed a clear negative correlation between $^{18}\Delta$ and COS uptake flux, with a larger change in $^{18}\Delta$ for C_3 species, compared to C_4. Figure 8 shows $^{18}\Delta$ against the COS uptake flux for our data. We do not observe such a correlation between $^{18}\Delta$ and the uptake COS flux. However, our range in COS uptake flux for each species is small, as we found that the COS uptake flux did not change significantly when adjusting the light intensity. In the same range of COS uptake flux data, Stimler et al. (2011) did not find a strong trend in $^{18}\Delta$ either.

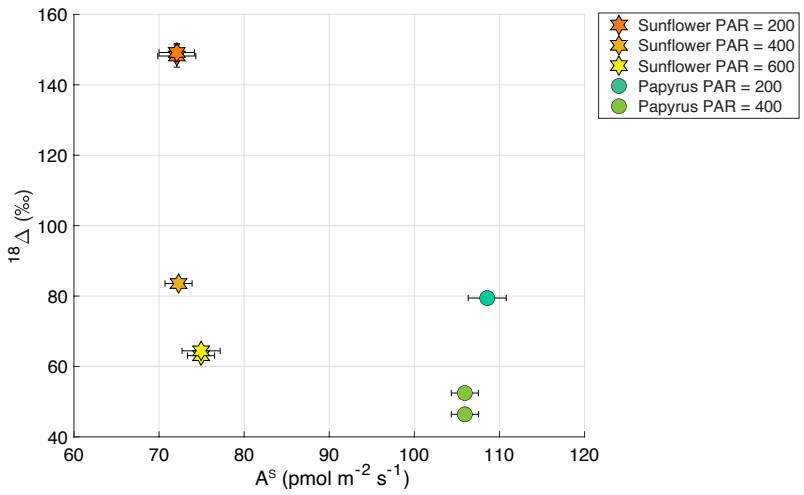

Figure 8. $^{18}\Delta$ (‰) plotted against A^S (COS uptake flux in pmol m^{-2} s^{-1}) for sunflower (C3) and papyrus (C4), where the different symbols and colors indicate the plant types and PAR (µmol m^{-2} s^{-1}).

4 Conclusion

This study presented measurements of COS and CO_2 plant uptake fluxes and isotope discrimination factors $^{34}\Delta$ of COS, $^{13}\Delta$ and $^{18}\Delta$ of CO_2 and for sunflower (C_3) and papyrus (C_4). The experiments were conducted using a flow-

https://doi.org/10.5194/egusphere-2025-215
Preprint. Discussion started: 10 February 2025

through gas exchange system, which is a new and different method compared to previously reported measurements of COS isotope fractionation during plant uptake (Davidson et al., 2021; 2022). The gas exchange system including the QCLS and LI-7000 instruments ensured stable chamber conditions, which were easy to monitor throughout the experiments.

Our study is the first to combine measurements of both COS and CO_2 plant isotope discrimination, where the CO_2 values provided additional information on the plant's behavior and their reactions to changes in environmental conditions. CO_2 assimilation increased with increasing PAR level, consistent with previous results under similar conditions. However, the moderate to low-light conditions were limiting CO_2 assimilation rate. Corresponding CO_2 isotope discrimination values, $^{13}\Delta$ and $^{18}\Delta$, were therefore higher at maximum capacity for CO_2 assimilation rate. CO_2 isotope discrimination as well as C_i^C/C_a^C were lower in papyrus than in sunflower, as expected and C_i^C/C_a^C decreased with light intensity for both species. Therefore, we conclude that both species were behaving normal, albeit not in the most optimal conditions for maximum capacity for photosynthetic CO_2 assimilation.

In contrast to photosynthesis, COS assimilation was light-independent, which is expected since the hydrolysis reaction catalyzed by CA does not require light. The observed COS uptake flux was lower during the dark experiments, but not zero, indicating some residual stomatal opening. Our measurements also showed a constant $^{34}\Delta$ across different light settings, which can be explained by the rather constant C_i^S/C_a^S and C_m^S/C_a^S values. Surprisingly, $^{34}\Delta$ also did not differ significantly between papyrus and sunflower, whereas previous measurements (Davidson et al., 2022) did show a higher ^{34}S isotope discrimination for C_4 species. However, C_i^S/C_a^S and C_m^S/C_a^S were also not different between our measured C_3 and C_4 species, hence similar isotope discrimination is expected. Nevertheless, our values for $^{34}\Delta$ are close to the previously reported values by Davidson et al. (2022), despite using a different experimental set-up and a different way to calculate the isotopic discrimination (Evans et al., 1986).

Appendices

Appendix A: Supplementary figures

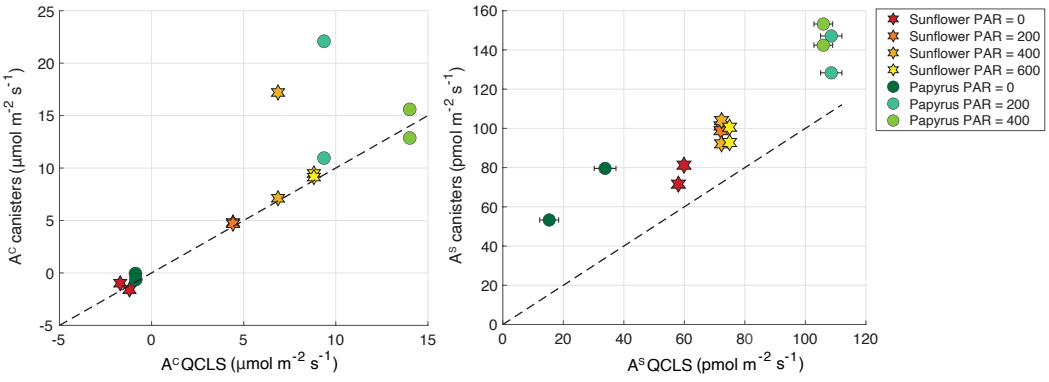

Figure A1. CO_2 and COS fluxes in µmol m^{-2} s^{-1} and pmol m^{-2} s^{-1}, respectively, calculated from the discrete samples that were analyzed on the mass spectrometer, plotted against the fluxes that were calculated from the online QCLS measurements. Uncertainty bars are ± 1σ, obtained using error propagation of the measurement errors on all the components used during the flux

https://doi.org/10.5194/egusphere-2025-215
Preprint. Discussion started: 10 February 2025

calculations (see supplementary materials). The errors are only depicted when they are larger than the symbols. The stars symbols are the sunflower data, and the circles are the papyrus data. The different color shadings indicate the varying PAR levels in µmol m^{-2} s^{-1}. The black dashed line shows the one-to-one line, for reference. The two samples that clearly fall off the line in the CO_2 plot were excluded from both the CO_2 and COS dataset, as these sample canisters had possibly leaked or were contaminated with air other than the plant chamber air.

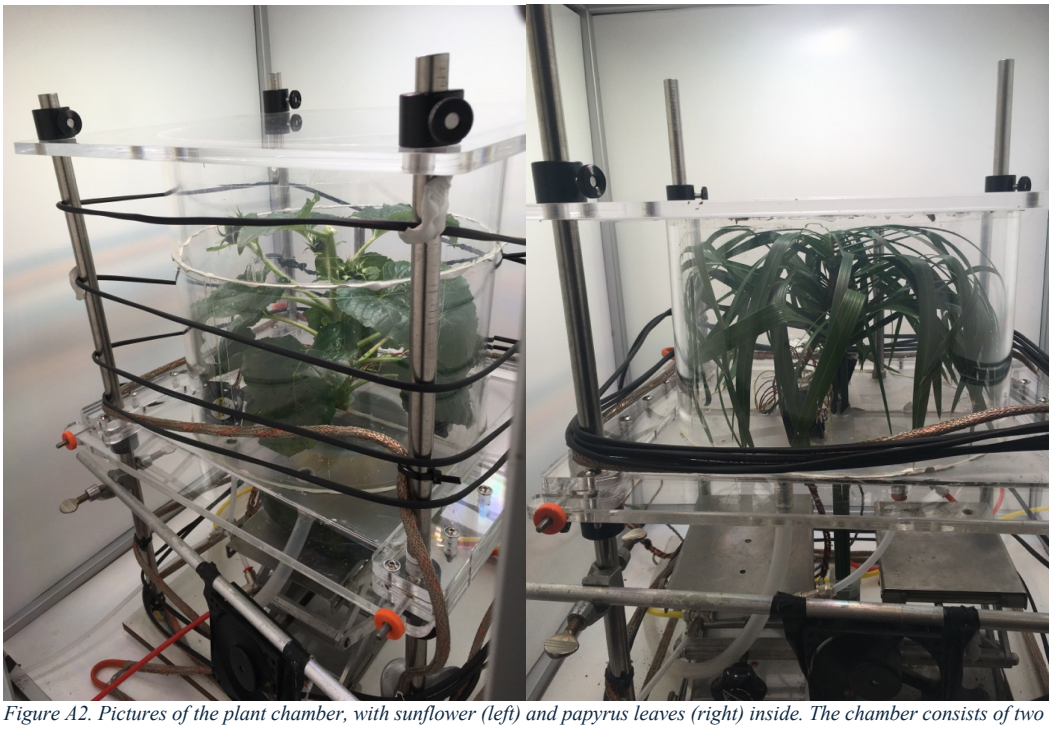

Figure A2. Pictures of the plant chamber, with sunflower (left) and papyrus leaves (right) inside. The chamber consists of two cylinders, connected to each other and to the upper and lower panels with Terostat RB VII. The plant pot and soil are kept outside of the chamber and the chamber is sealed onto the stem with Terostat as well. The black wires are automated (computer controlled) heating wires, ensuring constant temperature around the chamber.

Appendix B: Gas exchange calculations for CO_2 and COS

We detail gas exchange equations of von Caemmerer and Farquhar (1981) for CO_2 and adapt this theory to derive gas exchange parameters for COS. For assimilation rates and mixing ratios we adopt a nomenclature where the superscript *c* refers to CO_2 and *s* to COS. For conductances the subscript represents the molecule of interest (*w* – water, *c* – CO_2, *s* – COS) and the superscript the type of conductance (*t* – total, *b* – boundary layer, *s* – stomata).

<u>CO_2 and COS assimilation rates</u> (A^c , A^s, µmol CO_2 m^{-2} s^{-1}):

$$A^c = \frac{u_e}{S}\left(c_e^c - c_a^c\frac{1-w_e}{1-w_a}\right), \tag{B1}$$

$$A^s = \frac{u_e}{S}\left(c_e^s - c_a^s\frac{1-w_e}{1-w_a}\right), \tag{B2}$$

where u_e is the molar flow of air entering the chamber (mol air s^{-1}), S is the leaf area (m^2), c_e^c and c_a^c (µmol CO_2 mol air^{-1}) are the [CO_2] in the air entering and leaving the chamber, respectively, and c_e^s and c_a^s (pmol COS mol air^{-1}) are the [COS] in the air entering and leaving the chamber, respectively.

<u>Transpiration rate</u> (mol H_2O $m^{-2}s^{-1}$)

https://doi.org/10.5194/egusphere-2025-215
Preprint. Discussion started: 10 February 2025

$$E = \frac{u_e}{S}\frac{w_a - w_e}{1 - w_a}, \tag{B3}$$

where w_e, w_a (mol of H_2O mol air^{-1}) are the mole fractions of water vapor in the air *entering* the chamber and in the chamber *air* (which equals to the air *out* of the chamber).

Total conductance to water vapor (g_w^t, mol H_2O m^2 s^{-1}):

$$g_w^t = E\frac{1 - \frac{w_i + w_a}{2}}{w_i - w_a}, \tag{B4}$$

where (mol of H_2O mol air^{-1}) is the mole fraction of water vapor *inside* the leaf, which assuming saturation with water vapour at the leaf temperature (T_l, ºC) can be calculated:

$$w_i = \frac{0.61635e^{\frac{17.502T_l}{240.97+T_l}}}{P_a}, \tag{B5}$$

where P_a (kPa) is atmosphere pressure in the chamber.

Stomata conductance to water (g_s^w, mol H_2O m^{-2} s^{-1}) is:

$$g_s^w = \frac{1}{\frac{1}{g_t^w} - \frac{1}{g_b^w}}, \tag{B6}$$

where g_b^w is the boundary layer conductance to water, a characteristic of each plant chamber, but often very large in well stirred chambers (a requisite for gas exchange).

Total conductance to CO_2 (g_t^c, mol CO_2 m^{-2} s^{-1}) and COS (g_t^s, mol COS m^{-2} s^{-1}):

$$g_t^c = \frac{1}{\frac{1.6}{g_s^w} + \frac{1.37}{g_b^w}}, \tag{B7}$$

$$g_t^s = \frac{1}{\frac{1.94}{g_s^w} + \frac{1.56}{g_b^w}}, \tag{B8}$$

where the coefficient 1.6 and 1.37 (mol H_2O mol CO_2^{-1}) are the ratio of diffusivities of CO_2 to water vapor in air, and in the boundary layer, respectively. The coefficients 1.94 and 1.56 (mol H_2O mol COS^{-1}) are the ratio of diffusivities of COS to water vapor in air, and boundary layer, respectively (Fuller *et al.*, 1966; Farquhar & Lloyd, 1993).

Concentration inside the leaf of CO_2 (c_i^c, µmol CO_2 mol wet air^{-1}) and COS (c_i^s, pmol COS mol wet air^{-1})

A^c and A^s are determined with gas exchange with Eqs. (B1) and (B2), and can also be related to the [CO_2] and [COS] inside the leaf with the equations:

$$A^c = g_t^c(c_a^c - c_i^c) - E\frac{c_a^c + c_i^c}{2}, \tag{B9}$$

$$A^s = g_t^s(c_a^s - c_i^s) - E\frac{c_a^s + c_i^s}{2}, \tag{B10}$$

where $E\frac{c_a^c+c_i^c}{2}$ and $E\frac{c_a^s+c_i^s}{2}$ are ternary corrections that accounts for the influence of transpiration on the diffusion of CO_2 and COS into the leaf. Solving c_i^c from Eqn 9 and c_i^s from Eq. (B10) results in:

$$c_i^c = \frac{\left(g_t^c - \frac{E}{2}\right)c_a^c - A^c}{g_t^c + \frac{E}{2}}, \tag{B11}$$

https://doi.org/10.5194/egusphere-2025-215
Preprint. Discussion started: 10 February 2025

$$c_i^s = \frac{\left(g_t^s - \frac{E}{2}\right) c_a^s - A^s}{g_t^s + \frac{E}{2}}. \tag{B12}$$

COS concentration in the mesophyll at the sites of CA (c_m^s, pmol COS mol wet air^{-1}):

By analogy with the model for photosynthetic discrimination against $^{13}CO_2$ (Farquhar *et al.*, 1982; Farquhar & Cernusak, 2012) discrimination against $CO^{36}S$ (‰) during plant uptake can be described:

$$\Delta^{34}S = \frac{1}{1-t}\overline{a_{c_i^s}}\frac{c_a^s - c_i^s}{c_a^s} + \frac{1+t}{1-t}\left[a_m\frac{c_i^s - c_m^s}{c_a^s} + h\frac{c_m^s}{c_a^s}\right], \tag{B13}$$

where $\overline{a_{c_i^s}}$ (‰) is the weighted discrimination for diffusion across the leaf boundary layer and inside the mesophyll, calculated as:

$$\overline{a_{c_i^s}} = \frac{a_b(c_a^s - c_s^s) + a_s(c_s^s - c_i^s)}{c_a^s - c_i^s}, \tag{B14}$$

with c_s^s, the [COS] (pmol COS mol wet air^{-1}) at the leaf surface, is:

$$c_s^s = c_a^s - A^s\frac{1.56}{g_b^w}. \tag{B15}$$

The t is a ternary correction factor calculated as (Farquhar & Cernusak, 2012):

$$t = \alpha_{ac}\frac{E}{2g_t^s}, \tag{B16}$$

where $\alpha_{ac} = 1 + \frac{\overline{a_{c_i^s}}}{1000}$.

The a_b (= 3.5‰), a_s (= 5.2‰), and a_m (= 0.5‰) are fractionations for COS diffusion across the boundary layer, across the stomata, and due to COS dissolution and diffusion in water through the mesophyll, respectively (Davidson *et al.*, 2022). h (=15 ± 2‰) is the fractionation during COS hydrolysis by CA (Davidson *et al.*, 2022).

The c_m^s can be solved from Eqn 13 as:

$$c_m^s = \frac{(1-t)\cdot\Delta^{34}S\cdot c_a^s - \overline{a_{c_i^s}}(c_a^s - c_i^s) - (1+t)\cdot a_m\cdot c_i^s}{(1+t)(h-a_m)}. \tag{B17}$$

Because $t \cong 0$, then Eq. (B17) can be simplified to:

$$c_m^s \cong \frac{\Delta^{34}S\cdot c_a^s - \overline{a_{c_i^s}}(c_a^s - c_i^s) - a_m\cdot c_i^s}{h - a_m}. \tag{B18}$$

Substituting in Eq. (B18) the $\overline{a_{c_i^s}}$ for its expression given in Eq. (B14) and rearranging terms result in:

$$c_m^s \cong \frac{c_a^s(\Delta^{34}S - a_b) + c_s^s(a_b - a_s) + c_i^s(a_s - a_m)}{h - a_m} \tag{B19}$$

Substituting in Eq. (B19) the fractionation factors by their values results in:

$$c_m^s \cong \frac{(\Delta^{34}S - 3.5)c_a^s - 1.7c_s^s + 4.7c_i^s}{14.5}, \tag{B20}$$

where $\Delta^{34}S$ (‰) can be experimentally determined during measurements of gas exchange as (Evans *et al.*, 1986):

$$\Delta^{34}S = \frac{c_e^s}{c_e^s - c_o^s}\frac{\delta_o^{34} - \delta_e^{34}}{1 + \delta_o^{34} - \frac{c_e^s}{c_e^s - c_o^s}(\delta_o^{34} - \delta_e^{34})}, \tag{B21}$$

where c_e^s and c_o^s are the mole of COS in mole of *dry* air in the air *entering* and going *out* the chamber, and δ_e^{34} and δ_o^{34} (per mil) are the $\delta^{34}S$ isotope composition of the air entering and leaving the chamber, respectively. The term

https://doi.org/10.5194/egusphere-2025-215
Preprint. Discussion started: 10 February 2025

$\frac{c_e^s}{c_e^s - c_o^s}$ is often represented as ζ. The δ^{34}S values in the numerator should be divided by 1000 (for example if δ_o^{34} =10‰, then 0.0010 should be used).

We present c_m^s values calculated including ternary (Eq. (B17)). Ignoring ternary overestimated c_m^s ~1% at PAR = 200 and ~5% at PAR = 600.

Data availability

The dataset is available at: 10.5281/zenodo.14677494

Author contribution

Conceptualization: SLB, MCK, MEP, LW. Data curation: SLB. Formal analysis: SLB, NUL. Funding acquisition: MCK. Investigation: SLB, SMD, MW, LMJK, LM, AC, SH. Methodology: SLB, SMD, MW, LMJK, MEP. Resources: SMD, MW, LM, SH. Supervision: MEP, TR, MCK. Visualization: SLB, NUL. Writing – original draft preparation: SLB, NUL. Writing – review & editing: SMD, MW, LMJK, NUL, LM, MEP, AC, LW, TR, SH, MCK.

Competing interests

The authors declare that they have no conflict of interest

Acknowledgements

We are grateful for the technical support from Carina van der Veen, Marcel Portanger and Giorgio Cover. The authors gratefully acknowledge the insightful discussions with Jérôme Ogée.

Financial support

This project has received funding from the European Research Council (ERC) under the European Union's Horizon 2020 research and innovation program under grant agreement No 742798 (COS-OCS; to M. C. Krol)

References

Adnew, G. A., Pons, T. L., Koren, G., Peters, W., & Röckmann, T. (2020). Leaf-scale quantification of the effect of photosynthetic gas exchange on Δ 17 O of atmospheric CO 2. *Biogeosciences*, *17*(14), 3903-3922.

Angert, A., Said-Ahmad, W., Davidson, C., & Amrani, A. (2019). Sulfur isotopes ratio of atmospheric carbonyl sulfide constrains its sources. *Scientific reports*, *9*(1), 741.

Asaf, D., Rotenberg, E., Tatarinov, F., Dicken, U., Montzka, S. A., and Yakir, D. (2013). Ecosystem photosynthesis inferred from measurements of carbonyl sulphide flux. Nature Geoscience, 6(3):186–190.

Aubrey, D. P., & Teskey, R. O. (2009). Root-derived CO2 efflux via xylem stream rivals soil CO2 efflux. *New Phytologist*, *184*(1), 35-40.

Baartman, S. L., Krol, M. C., Röckmann, T., Hattori, S., Kamezaki, K., Yoshida, N., & Popa, M. E. (2021). A GC-IRMS method for measuring sulfur isotope ratios of carbonyl sulfide from small air samples. *Open Research Europe*, *1*.

https://doi.org/10.5194/egusphere-2025-215
Preprint. Discussion started: 10 February 2025

Billesbach, D. P., Berry, J. A., Seibt, U., Maseyk, K., Torn, M. S., Fischer, M. L., ... & Campbell, J. E. (2014). Growing season eddy covariance measurements of carbonyl sulfide and CO2 fluxes: COS and CO2 relationships in Southern Great Plains winter wheat. *Agricultural and Forest Meteorology*, *184*, 48-55.

Bloemen, J., McGuire, M. A., Aubrey, D. P., Teskey, R. O., & Steppe, K. (2013). Transport of root-respired CO2 via the transpiration stream affects aboveground carbon assimilation and CO2 efflux in trees. *New Phytologist*, *197*(2), 555-565.

Brenninkmeijer, C. A. M.: Measurement of the abundance of 14CO in the atmosphere and the 13C / 12C and 18O/16O ratio of atmospheric CO with applications in New Zealand and Antarctica, J. Geophys. Res., 98, 10595–10614, doi:10.1029/93JD00587, 1993.

Buck, A. L. (1981). New equations for computing vapor pressure and enhancement factor. *Journal of Applied Meteorology (1962-1982)*, 1527-1532.

von Caemmerer, S. V., & Farquhar, G. D. (1981). Some relationships between the biochemistry of photosynthesis and the gas exchange of leaves. *Planta*, *153*, 376-387.

Cerling, T. E., Harris, J. M., MacFadden, B. J., Leakey, M. G., Quade, J., Eisenmann, V., & Ehleringer, J. R. (1997). Global vegetation change through the Miocene/Pliocene boundary. *Nature*, *389*(6647), 153-158.

Cernusak, L. A., Ubierna, N., Winter, K., Holtum, J. A., Marshall, J. D., & Farquhar, G. D. (2013). Environmental and physiological determinants of carbon isotope discrimination in terrestrial plants. *New Phytologist*, *200*(4), 950-965.

Cho, A., Kooijmans, L. M., Kohonen, K. M., Wehr, R., & Krol, M. C. (2023). Optimizing the carbonic anhydrase temperature response and stomatal conductance of carbonyl sulfide leaf uptake in the Simple Biosphere model (SiB4). *Biogeosciences*, *20*(13), 2573-2594.

Commane, R., Meredith, L. K., Baker, I. T., Berry, J. A., Munger, J. W., Montzka, S. A., ... & Wofsy, S. C. (2015). Seasonal fluxes of carbonyl sulfide in a midlatitude forest. *Proceedings of the National Academy of Sciences*, *112*(46), 14162-14167.

Davidson, C., Amrani, A., & Angert, A. (2021). Tropospheric carbonyl sulfide mass balance based on direct measurements of sulfur isotopes. *Proceedings of the National Academy of Sciences*, *118*(6), e2020060118.

Davidson, C., Amrani, A., and Angert, A. (2022). Carbonyl sulfide sulfur isotope fractionation during uptake by C3 and C4 plants. Journal of Geophysical Research: Biogeosciences, 127(10):e2022JG007035.

Eggels, S., Blankenagel, S., Schön, C. C., & Avramova, V. (2021). The carbon isotopic signature of C4 crops and its applicability in breeding for climate resilience. *Theoretical and Applied Genetics*, *134*(6), 1663-1675.

Ellsworth, P. Z., & Cousins, A. B. (2016). Carbon isotopes and water use efficiency in C4 plants. *Current Opinion in Plant Biology*, *31*, 155-161.

Evans, J. R., Sharkey, T. D., Berry, J. A., & Farquhar, G. D. (1986). Carbon isotope discrimination measured concurrently with gas exchange to investigate CO2 diffusion in leaves of higher plants. *Functional Plant Biology*, *13*(2), 281-292.

Farquhar, G. D. (1983). On the nature of carbon isotope discrimination in C4 species. *Functional Plant Biology*, *10*(2), 205-226.

Farquhar, G. D., von Caemmerer, S. V., & Berry, J. A. (1980). A biochemical model of photosynthetic CO_2 assimilation in leaves of C 3 species. *planta*, *149*, 78-90.

https://doi.org/10.5194/egusphere-2025-215
Preprint. Discussion started: 10 February 2025

Farquhar, G. D., & Cernusak, L. A. (2012). Ternary effects on the gas exchange of isotopologues of carbon dioxide. *Plant, Cell & Environment*, *35*(7), 1221-1231.

Farquhar, G. D., Ehleringer, J. R., & Hubick, K. T. (1989). Carbon isotope discrimination and photosynthesis. *Annual review of plant physiology and plant molecular biology*, *40*(1), 503-537.

Farquhar, G. D., O'Leary, M. H., & Berry, J. A. (1982). On the relationship between carbon isotope discrimination and the intercellular carbon dioxide concentration in leaves. *Functional Plant Biology*, *9*(2), 121-137.

Farquhar, G. D., & Lloyd, J. (1993). Carbon and oxygen isotope effects in the exchange of carbon dioxide between terrestrial plants and the atmosphere. In *Stable isotopes and plant carbon-water relations* (pp. 47-70). Academic Press.

Farquhar, G. D., Lloyd, J., Taylor, J. A., Flanagan, L. B., Syvertsen, J. P., Hubick, K. T., ... & Ehleringer, J. R. (1993). Vegetation effects on the isotope composition of oxygen in atmospheric CO2. *Nature*, *363*(6428), 439-443.

Francey, R. J. and Tans, P. P.: Latitudinal variation in oxygen-18 of atmospheric CO2, Nature, 327, 2 pp., 1987.

Fuller, E. N., Schettler, P. D., & Giddings, J. C. (1966). New method for prediction of binary gas-phase diffusion coefficients. *Industrial & Engineering Chemistry*, *58*(5), 18-27.

Gillon, J. S., & Yakir, D. (2000). Naturally low carbonic anhydrase activity in C4 and C3 plants limits discrimination against C18OO during photosynthesis. *Plant, Cell & Environment*, *23*(9), 903-915.

Gentsch, L., Sturm, P., Hammerle, A., Siegwolf, R., Wingate, L., Ogée, J., ... & Knohl, A. (2014). Carbon isotope discrimination during branch photosynthesis of Fagus sylvatica: field measurements using laser spectrometry. *Journal of experimental botany*, *65*(6), 1481-1496.

Kohn, M. J. (2010). Carbon isotope compositions of terrestrial C3 plants as indicators of (paleo) ecology and (paleo) climate. *Proceedings of the National Academy of Sciences*, *107*(46), 19691-19695.

Kooijmans, L. M., Maseyk, K., Seibt, U., Sun, W., Vesala, T., Mammarella, I., Kolari, P., Aalto, J., Franchin, A., Vecchi, R., et al. (2017). Canopy uptake dominates nighttime carbonyl sulfide fluxes in a boreal forest. Atmospheric Chemistry and Physics, 17(18):11453–11465.

Kooijmans, L. M., Sun, W., Aalto, J., Erkkilä, K.M., Maseyk, K., Seibt, U., Vesala, T., Mammarella, I., and Chen, H. (2019). Influences of light and humidity on carbonyl sulfide-based estimates of photosynthesis. Proceedings of the National Academy of Sciences, 116(7):2470– 2475.

Kromdijk, J., Griffiths, H., & Schepers, H. E. (2010). Can the progressive increase of C4 bundle sheath leakiness at low PFD be explained by incomplete suppression of photorespiration? *Plant, cell & environment*, *33*(11), 1935-1948.

Kubásek, J., Urban, O., & Šantrůček, J. (2013). C4 plants use fluctuating light less efficiently than do C3 plants: a study of growth, photosynthesis and carbon isotope discrimination. *Physiologia plantarum*, *149*(4), 528-539.

Lazzarin, M., Dupont, K., van Ieperen, W., Marcelis, L. F., & Driever, S. M. (2024). Far-red light effects on plant photosynthesis: from short-term enhancements to long-term effects of artificial solar light. *Annals of Botany*, mcae104.

Lai, J., Kooijmans, L. M., Sun, W., Lombardozzi, D., Campbell, J. E., Gu, L., ... & Sun, Y. (2024). Terrestrial photosynthesis inferred from plant carbonyl sulfide uptake. *Nature*, 1-7.

Li, M., & Jones, M. B. (1995). CO2 and O2 transport in the aerenchyma of Cyperus papyrus L. *Aquatic Botany*, *52*(1-2), 93-106.

https://doi.org/10.5194/egusphere-2025-215
Preprint. Discussion started: 10 February 2025

Maignan, F., Abadie, C., Remaud, M., Kooijmans, L. M., Kohonen, K. M., Commane, R., ... & Peylin, P. (2021). Carbonyl sulfide: comparing a mechanistic representation of the vegetation uptake in a land surface model and the leaf relative uptake approach. *Biogeosciences*, *18*(9), 2917-2955.

Pengelly, J. J., Sirault, X. R., Tazoe, Y., Evans, J. R., Furbank, R. T., & Von Caemmerer, S. (2010). Growth of the C4 dicot Flaveria bidentis: photosynthetic acclimation to low light through shifts in leaf anatomy and biochemistry. *Journal of experimental botany*, *61*(14), 4109-4122.

Plowman, A. B. (1906). The comparative anatomy and phylogeny of the Cyperaceae. *Annals of Botany*, *20*(77), 1-33.

Protoschill-Krebs, G., & Kesselmeier, J. (1992). Enzymatic pathways for the consumption of carbonyl sulphide (COS) by higher plants. *Botanica Acta*, *105*(3), 206-212.

Protoschill-Krebs, G., Wilhelm, C., & Kesselmeier, J. (1996). Consumption of carbonyl sulphide (COS) by higher plant carbonic anhydrase (CA). *Atmospheric Environment*, *30*(18), 3151-3156.

Seibt, U., Wingate, L., Berry, J. A., & Lloyd, J. (2006). Non-steady state effects in diurnal 18O discrimination by Picea sitchensis branches in the field. *Plant, Cell & Environment*, *29*(5), 928-939.

Spielmann, F. M., Hammerle, A., Kitz, F., Gerdel, K., Alberti, G., Peressotti, A., ... & Wohlfahrt, G. (2023). On the variability of the leaf relative uptake rate of carbonyl sulfide compared to carbon dioxide: Insights from a paired field study with two soybean varieties. *Agricultural and Forest Meteorology*, *338*, 109504.

Stimler, K., Berry, J. A., Montzka, S. A., and Yakir, D. (2011). Association between carbonyl sulfide uptake and 18Δ during gas exchange in C3 and C4 leaves. Plant physiology, 157(1):509 517.

Stimler, K., Berry, J. A., & Yakir, D. (2012). Effects of carbonyl sulfide and carbonic anhydrase on stomatal conductance. *Plant Physiology*, *158*(1), 524-530.

Sun, W., Maseyk, K., Lett, C., & Seibt, U. (2024). Restricted internal diffusion weakens transpiration–photosynthesis coupling during heatwaves: Evidence from leaf carbonyl sulphide exchange. *Plant, Cell & Environment*, *47*(5), 1813-1833.

Tezara, W., Driscoll, S., & Lawlor, D. W. (2008). Partitioning of photosynthetic electron flow between CO_2 assimilation and O_2 reduction in sunflower plants under water deficit. *Photosynthetica*, *46*, 127-134.

Ubierna, N., Sun, W. E. I., Kramer, D. M., & Cousins, A. B. (2013). The efficiency of C4 photosynthesis under low light conditions in Zea mays, Miscanthus x giganteus and Flaveria bidentis. *Plant, cell & environment*, *36*(2), 365-381.

Vesala, T., Kohonen, K. M., Kooijmans, L. M., Praplan, A. P., Foltýnová, L., Kolari, P., ... & Mammarella, I. (2022). Long-term fluxes of carbonyl sulfide and their seasonality and interannual variability in a boreal forest. *Atmospheric Chemistry and Physics*, *22*(4), 2569-2584.

Wehr, R., Commane, R., Munger, J. W., McManus, J. B., Nelson, D. D., Zahniser, M. S., Saleska, S. R., and Wofsy, S. C. (2017). Dynamics of canopy stomatal conductance, transpiration, and evaporation in a temperate deciduous forest, validated by carbonyl sulfide uptake. Biogeosciences, 14(2):389–401.

Whelan, M. E., Lennartz, S. T., Gimeno, T. E., Wehr, R., Wohlfahrt, G., Wang, Y., Kooijmans, L. M., Hilton, T. W., Belviso, S., Peylin, P., et al. (2018). Reviews and syntheses: Carbonyl sulfide as a multi-scale tracer for carbon and water cycles. Biogeosciences, 15(12):3625– 3657.
Wingate, L., Ogée, J., Burlett, R., Bosc, A., Devaux, M., Grace, J., Loustau, D., and Gessler, A. (2010). Photosynthetic carbon isotope discrimination and its relationship to the carbon isotope signals of stem, soil and ecosystem respiration. New Phytologist, 188(2):576–589.

https://doi.org/10.5194/egusphere-2025-215
Preprint. Discussion started: 10 February 2025

Wingate, L., Seibt, U., Moncrieff, J. B., Jarvis, P. G., & Lloyd, J. O. N. (2007). Variations in 13C discrimination during CO2 exchange by Picea sitchensis branches in the field. *Plant, Cell & Environment*, *30*(5), 600-616.

Wohlfahrt, G., Brilli, F., Hörtnagl, L., Xu, X., Bingemer, H., Hansel, A., and Loreto, F. (2012). Carbonyl sulfide (COS) as a tracer for canopy photosynthesis, transpiration and stomatal conductance: potential and limitations. Plant, cell & environment, 35(4):657–667.

Wohlfahrt, G., Hammerle, A., Spielmann, F. M., Kitz, F., & Yi, C. (2023). Novel estimates of the leaf relative uptake rate of carbonyl sulfide from optimality theory. *Biogeosciences*, *20*(3), 589-596.

Yakir, D.: Oxygen-18 of leaf water: a crossroad for plant-associated isotopic signals, in: Stable isotopes: integration of biological, ecological and geochemical processes, edited by: Griffiths, H., BIOS Scientific Publishers, Oxford, 147–188, 1998.